

# A high resolution fundamental frequency determination based on phase changes of the Fourier transform

Judith C. Brown

*Physics Department, Wellesley College, Wellesley, Massachusetts 01281 and Media Lab, Massachusetts Institute of Technology, Cambridge, Massachusetts 02139*

Miller S. Puckette

*IRCAM, 31 rue St Merri, Paris 75004, France*

(Received 16 June 1992; revised 5 April 1993; accepted 6 April 1993)

The constant  $Q$  transform described recently [J. C. Brown and M. S. Puckette, "An efficient algorithm for the calculation of a constant  $Q$  transform," *J. Acoust. Soc. Am.* **92**, 2698–2701 (1992)] has been adapted so that it is suitable for tracking the fundamental frequency of extremely rapid musical passages. For this purpose the calculation described previously has been modified so that it is constant frequency resolution rather than constant  $Q$  for lower frequency bins. This modified calculation serves as the input for a fundamental frequency tracker similar to that described by Brown [J. C. Brown, "Musical fundamental frequency tracking using a pattern recognition method," *J. Acoust. Soc. Am.* **92**, 1394–1402 (1992)]. Once the fast Fourier transform (FFT) bin corresponding to the fundamental frequency is chosen by the frequency tracker, an approximation is used for the phase change in the FFT for a time advance of one sample to obtain an extremely precise value for this frequency. Graphical examples are given for musical passages by a violin executing vibrato and glissando where the fundamental frequency changes are rapid and continuous.

PACS numbers: 43.75.Yy, 43.60.Gk

## INTRODUCTION

Our fundamental frequency tracker is based upon the calculation of a constant  $Q$  spectral transform described recently by Brown and Puckette (1992). Here we showed that the direct calculation of the components of a constant  $Q$  transform can be accomplished more efficiently by a transformation of the fast Fourier transform (FFT). To summarize that calculation, the direct calculation can be carried out using

$$X^{cq}[k_{cq}] = \sum_{n=0}^{N[k_{cq}]-1} w[n, k_{cq}] x[n] e^{-j\omega_{k_{cq}} n},$$

where  $X^{cq}[k_{cq}]$  is the  $k_{cq}$  component of the constant  $Q$  transform,  $w[n, k_{cq}]$  is a window function of length  $N[k_{cq}]$ ,  $x[n]$  is a sampled function of time, and  $\omega_{k_{cq}}$  is the frequency of this component.

This can be evaluated using the following form of Parseval's equation

$$\sum_{n=0}^{N-1} x[n] \mathcal{H}^*[n, k_{cq}] = \frac{1}{N} \sum_{k=0}^{N-1} X[k] K^*[k, k_{cq}],$$

if we define

$$w[n, k_{cq}] e^{-j\omega_{k_{cq}} n} = \mathcal{H}^*[n, k_{cq}].$$

Since the functions  $\mathcal{H}^*[n, k_{cq}]$  have very few nonzero components, the fast Fourier transform  $X[k]$  of the signal  $x[n]$  can be transformed into a constant  $Q$  transform with very few additional operations.

For application to the performance of modern computer music, which includes extremely rapid passages, a

time resolution of 25 ms or less is desirable. We are thus confronted with the usual dilemma in choosing an acceptable trade-off between temporal and frequency resolution.

Our compromise consists of limiting the temporal extent of the window. This means that the low-frequency bins of our transform are constant frequency resolution (equal to the sample rate over the temporal window length) rather than constant  $Q$ . For example, we may choose for the center frequencies of the bins of the transform to correspond to the frequencies of notes of the equal tempered musical scale beginning with the first bin at  $C_3$  (130.9 Hz). Then a window length of 25 ms means that the resolution is a constant equal to 40 Hz (while the  $Q$  is variable) up to a frequency of 717.8 Hz or the 30th bin. The resolution is then variable with  $Q$  constant equal roughly 17 up to a frequency of 5274 Hz or the 65th bin. We will call this transform the modified constant  $Q$  transform, and we will show that limiting the temporal extent of the window for the low-frequency bins does not lead to decreased performance for the detection of the fundamental frequency. It does, of course, mean greater spillover for the low-frequency bins.

An example of this calculation can be found in Fig. 1 for a clarinet playing a chromatic scale where we have plotted the amplitude of the modified constant  $Q$  transform components against bin number in each frame. Time is increasing vertically for these frames. Here the lower  $Q$ 's (with the lowest value about 5) of the low-frequency bins are manifested by a greater bandwidth. This figure can be compared to Fig. 4 of Brown and Puckette (1992) for a spectrum of the same sound calculated with a "true" con-

## CLARINET SCALE

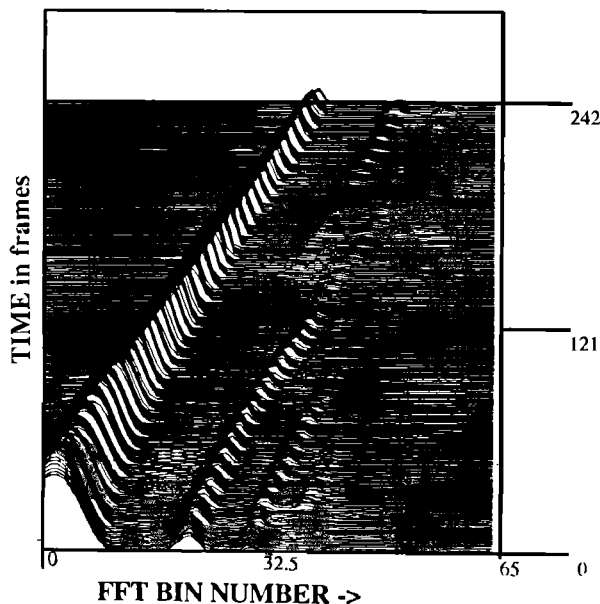


FIG. 1. Amplitude of the modified constant  $Q$  spectral components plotted against bin number (corresponding to frequency) for a series of time frames. A clarinet with microphone placed in the barrel is playing several octaves of a chromatic scale.

stant  $Q$  of 17. It is interesting to note that the even harmonics are missing as predicted for a clarinet up to about the 29th bin and at this point the energy in the third harmonic begins to decrease. The clarinet sound was recorded with the microphone in the barrel of the instrument so the spectrum is not as rich as for a normal clarinet sound.

### I. CALCULATION OF INITIAL FREQUENCY ESTIMATE

When the constant  $Q$  transform of a sound consisting of harmonic frequency components is plotted against log frequency, the spacing of these components is invariant (Brown, 1991). The fundamental frequency can then be determined by finding the position in log frequency space of this invariant pattern. This is best accomplished by calculating the cross-correlation function of each frame of the log frequency spectrum with the ideal pattern as discussed by Brown (1992).

The "ideal pattern" used in calculating the cross-correlation function consists of components with the frequency spacing discussed above and with amplitudes decreasing linearly from 1 for the fundamental to 0.6 for the highest harmonic. The purpose of varying the amplitudes is to prevent the choice of the frequency an octave below that of the true fundamental. For this position of the ideal pattern, all even components of the ideal pattern line up with components present in the spectrum. This is because the spacing of components  $2f$ ,  $4f$ ,  $6f$ , etc. is the same as that of components  $f$ ,  $2f$ ,  $3f$ , etc. If all components are weighted equally, the value of the cross-correlation function will have the same value for even components of the pattern aligned with the components of the signal as for the "true" position where all components of the pattern fall on

## VIOLIN SCALE

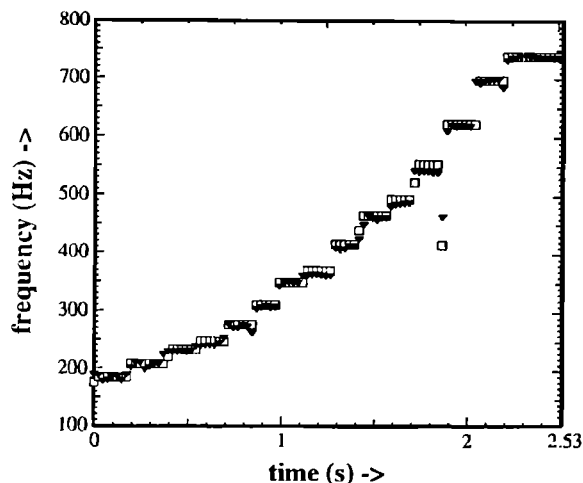


FIG. 2. Frequency tracking results for a violin playing two octaves of a diatonic scale. The open square is the result from the modified constant  $Q$  fundamental frequency tracker. The solid triangle is the precise frequency returned by the high-resolution phase calculation.

their counterparts in the test spectrum. However, with smaller weights on higher components, this error is avoided.

We have estimated the run time for our algorithm with calculations carried out on a 40-MHz Intel i860 using a hand-coded routine. With a 512-point FFT and quarter tone spacing over three octaves, the FFT takes  $343 \mu\text{s}$  and the transform  $166 \pm 2 \mu\text{s}$  (measured on an oscilloscope). The cross-correlation calculation involves well under 250 multiplies even with ten components in the harmonic pattern so the computation time for this operation is negligible. The overall computation time then is on the order of 0.5 ms. This can be compared to a time advance of 25 ms between frames, so the calculation is easily carried out in real time.

Results of our calculation applied to digitized violin and clarinet scales are found in Figs. 2 and 3 where the open squares correspond to the frequencies of the notes of the equal tempered scale chosen by our frequency tracker plotted against frame number. The solid triangles will be explained in the next section. Each frame corresponds to a time advance of 25 ms in the sound. These are examples of instruments with very different spectra. The violin has a complex spectrum with many higher harmonics present. This clarinet sound was recorded with the microphone in the barrel and has a relatively simple spectrum with a smaller number of harmonics. The number of components in the ideal pattern used for the cross correlation varied accordingly, with 10 components for the violin and three components for the clarinet. There were essentially no errors in determining fundamental frequencies of the notes present with our modified constant  $Q$  transform.

### II. HIGH-RESOLUTION FREQUENCY DETERMINATION

#### A. Phase background

The importance of the phase in the discrete Fourier transform (DFT) has been discussed by Oppenheim and

## CLARINET SCALE

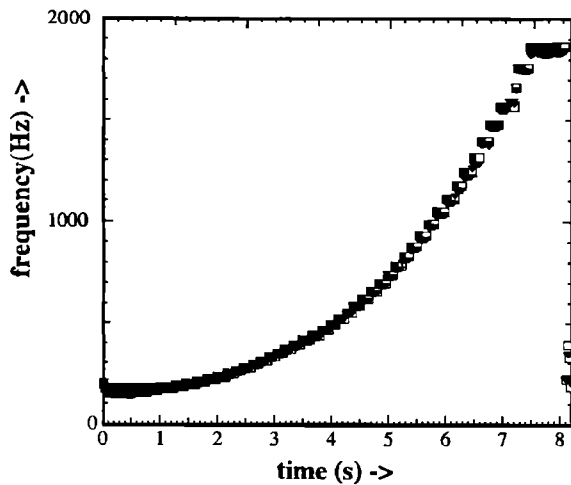


FIG. 3. Frequency tracking results for a clarinet playing several octaves of a chromatic scale. The open square is the result from the modified constant  $Q$  fundamental frequency tracker. The solid triangle is the precise frequency returned by the high-resolution phase calculation.

Luis (1981). They point out that in a variety of disciplines phase only information leads to a more recognizable reconstruction of the original object analyzed than does information based on magnitude only. Friedman (1985) demonstrated that one can obtain narrower formant bands for sonograms of speech using a histogram of occurrences against frequency with the frequency obtained from the time derivative of the phase of the short-time Fourier transform. Computationally this was obtained by calculating two short-time Fourier transform (STFT's) with the derivative of the window function used in one of them.

Earlier, in work on the phase vocoder applied to speech signals Flanagan and Golden (1966) used phase differences to obtain greater accuracy of Fourier components. Beauchamp (1966, 1969) and Grey and Moorer (1977) used a similar technique applied to musical signals. See also Moorer (1978) and Dolson (1986).

Charpentier (1986) described a pitch tracker based on frequencies obtained from an approximation for the phase difference of time frames of the STFT separated by one sample. We obtained this same expression independently and will discuss it in the following section.

### B. Phase calculation

The method of frequency determination which we have described in the Introduction and in Brown (1992) works extremely well for instruments playing discrete notes belonging to the equal tempered scale. Here the smallest frequency difference between notes is approximately 6%, and the results are reported as notes of the equal tempered scale. However, a very different situation can arise in passages played by stringed instruments or wind instruments. These instruments are not constrained to play discrete notes as are keyboard instruments. Thus the frequency can vary continuously as in, for example, a glissando or vibrato. Keyboard instruments may also be

tuned to temperaments other than equal tempered. For all of these cases the frequency determination must be much more accurate than 6% in order to track the audio waveform.

The frequency of a particular Fourier component as obtained from the bin into which it falls in the magnitude spectrum is only as accurate as the frequency difference between bins, in our case 6% or 3% depending on the calculation. This estimate can be improved by a quadratic fit using the amplitudes of the bin containing the maximum and the two adjacent bins and identifying the position of the maximum of the parabola thus obtained. This is an extremely well-known technique described recently by Smith and Serra (1987). We will discuss the accuracy of this approximation in a later section.

Even more accurate is a method we have developed based on an approximation for the phase change per unit sample for the Fourier component chosen as the correct fundamental frequency by our frequency tracker. It is well known that the frequency as determined by the change in phase is much more accurate than that obtained from the magnitude spectrum. However, the problem with determining the frequency from the phase difference over a reasonable hop size (samples between frames) is one of phase unwrapping. The phase change is only known modulo  $2\pi$ . This problem does not arise with a hop size of one sample since the highest digital frequency is  $\pi$  radians/sample, but this case necessitates the computation of an additional FFT.

In fact this additional computation can be avoided by using an approximation which assumes that  $x[n]$  is periodic. The phase change for a hop size of one sample can be obtained from the following identity (Oppenheim and Schaffer, 1975; Charpentier, 1986). If  $\mathcal{F}\{x[n]\}=X[k]$  is the  $k$ th component of the discrete Fourier transform of  $x[n]$ , then

$$\mathcal{F}\{x[n+m]\} \cong e^{j2\pi km/N} X[k] \quad (1)$$

is the DFT after  $m$  samples.

The above equation applies to an unwrapped DFT. It is possible to use this result to obtain a Hanning-windowed transform since the effect of windowing can be calculated in the frequency domain for this window. We will use the notation  $X^H[k]$  to denote the Hanning-windowed Fourier transform evaluated for a window beginning on sample  $n_0$ , that is

$$X^H[k, n_0] = \sum_{n=0}^{N-1} x[n+n_0] w[n] e^{-j2\pi kn/N},$$

where

$$\begin{aligned} w[n] &= \frac{1}{2} - \frac{1}{2} \cos(2\pi n/N) \\ &= 1/2 [1 - (\frac{1}{2})e^{j2\pi n/N} - \frac{1}{2}e^{-j2\pi n/N}]. \end{aligned}$$

Substituting this expression for the window in the preceding equation leads to

$$X^H[k, n_0] = \frac{1}{2} \{X[k] - \frac{1}{2}X[k+1] - \frac{1}{2}X[k-1]\}. \quad (2)$$

Using Eq. (1) with  $m=1$  in Eq. (2), the approximation for the Hanning-windowed DFT after one sample is

$$X^H[k, n_0+1] = \frac{1}{2} \{ e^{j2\pi k/N} X[k] - \frac{1}{2} e^{j2\pi(k+1)/N} X[k+1] - \frac{1}{2} e^{j2\pi(k-1)/N} X[k-1] \}.$$

And finally

$$X^H[k, n_0+1] = \frac{1}{2} e^{j2\pi k/N} \{ X[k] - \frac{1}{2} e^{j2\pi/N} X[k+1] - \frac{1}{2} e^{-j2\pi/N} X[k-1] \} \quad (3)$$

The digital frequency in radians per sample for the  $k$ th bin corresponding to the phase difference for a time advance of one sample is

$$\omega(k, n_0) = \phi(k, n_0+1) - \phi(k, n_0), \quad (4)$$

where

$$\phi(k, n_0+1) = \arctan \left\{ \frac{\text{Im}(X^H[k, n_0+1])}{\text{Re}(X^H[k, n_0+1])} \right\}$$

and

$$\phi(k, n_0) = \arctan \left\{ \frac{\text{Im}(X^H[k, n_0])}{\text{Re}(X^H[k, n_0])} \right\}.$$

This expression for the phase difference holds for any DFT bin with the bin indicated by  $k$ . For use with a fundamental frequency tracker, the calculation would only be used on the bin selected as winner by the tracker.

### III. RESULTS

To check this method a test file was generated in software consisting of the superposition of sinusoidal components of equal amplitude at frequencies 434.97, 1739.88, and 3479.77 Hz. These frequencies were chosen to fall into bin positions 10.1, 40.4, and 80.8. A 256-point DFT was taken, and the real and imaginary components obtained were substituted into Eq. (4) using the definitions following this equation. The calculation was carried out for each of the 128 positive frequency components of the DFT.

The result is found in Fig. 4 where we have plotted  $\omega(k)$  (converted to Hertz for a sample rate of 11025) against bin number. Note that the calculated frequencies are correct for five or more bins on either side of the bin into which the frequency belongs. This point will be discussed further in the section comparing this method with the phase vocoder.

The measured frequencies as determined by Eq. (4) were also printed out and were correct to the two decimal places indicated above. The solid diagonal line represents the center frequency of these DFT bins plotted against bin number. The analogous graph obtained from an exact measurement of  $\omega$  based on the calculation of two successive DFT's with a time advance of one sample was identical to this graph and is not included. This means that the assumption of periodicity used in Eq. (1) is extremely good for a hop size of 1 sample.

When used as the back end of a fundamental frequency tracker, the determination of the precise frequency

### TEST FILE WITH THREE SINUSOIDS

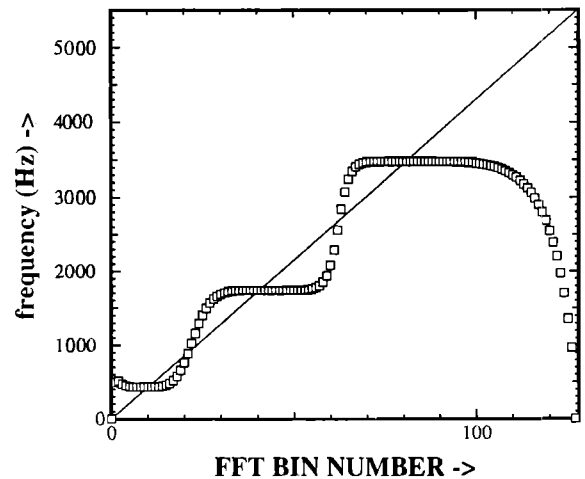


FIG. 4. High-resolution frequency as calculated in Eq. (4) for each bin plotted against bin number for a test file with three components.

as described adds a negligible amount to the computation time since it is only carried out for one DFT bin. Once the bin number for the initial estimate of the fundamental frequency is selected from the constant  $Q$  transform, a calculation is made to determine the corresponding bin number for the FFT. The real and imaginary parts of the FFT for this bin and those on either side of it were previously calculated, and only these three complex numbers are needed for the evaluation of Eqs. (2) and (3). These are then used in Eq. (4) with the definitions following it.

The precise frequencies were calculated for the violin and clarinet scales discussed previously. The results are given by the closed triangles in Figs. 2 and 3. Note that for the violin the precise frequency is correct in several cases where the initial estimate was off by a bin. For the clarinet in Fig. 3, the precise frequency is correct for the first three notes where the initial estimate was incorrect because the constant  $Q$  transform did not extend to that low a frequency.

The power of this method is even more apparent when it is applied to the acoustic sounds for which it is intended. In Figs. 5 and 6 are found the frequencies (solid triangles) obtained using Eq. (4) on the output from the frequency tracker described in Sec. I. A violin is executing a glissando in Fig. 5 and vibrato in Fig. 6. For comparison we include the open squares indicating the results for the frequency tracker without the phase correction. For the glissando two points on the precise frequency curve are slightly off, but these errors are small. We are uncertain as to their origin.

### IV. COMPARISON OF ACCURACY OF PHASE METHOD WITH QUADRATIC FIT

For a sampled function  $y(x)$  where values are only known for integral  $x$ , the position of the "true" maximum of the function usually occurs at nonintegral values of  $x$ . One widely used means of approximating the (noninte-

## VIOLIN GLISSANDO

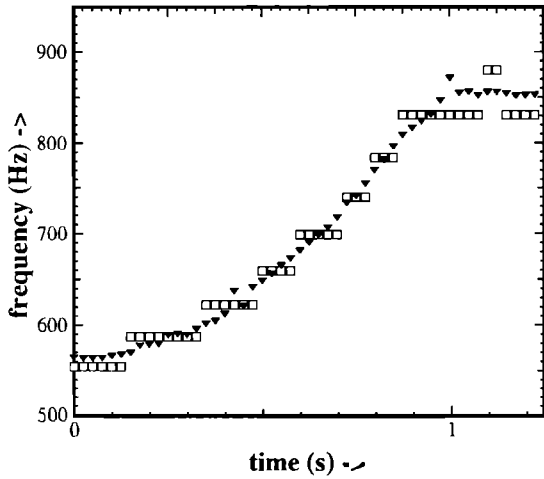


FIG. 5. High-resolution frequency plotted against time for a violin executing a glissando. Open squares represent the results of the fundamental frequency tracker with solid triangles the high-resolution results.

gral)  $x$  value where the true maximum occurs is by fitting a parabola through the point where the maximum of the sampled function occurs and the points on either side.

If the maximum occurs at  $x=0$  and  $y(0)=y_0$ , then the three points  $(-1, y_{-1})$ ,  $(0, y_0)$ , and  $(1, y_{+1})$  labeled with their  $x$  and  $y$  values are assumed to lie on a parabola. With a little algebra it is easy to show that the maximum of the parabola occurs at

$$x = \frac{y_{+1} - y_{-1}}{2(y_0 - y_{+1} - y_{-1})}. \quad (5)$$

The accuracy for the quadratic fit method can be calculated exactly for an input signal consisting of a single harmonic component. For a component falling into bin  $k_0$  with a frequency corresponding exactly to  $k_0+r$  where  $-0.5 \leq r \leq 0.5$  we evaluate Eq. (2)

## VIOLIN VIBRATO

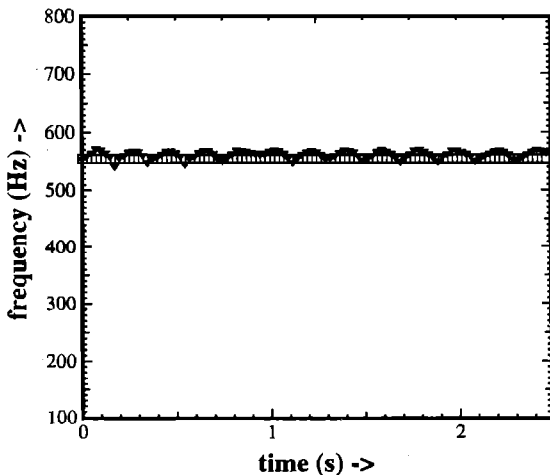


FIG. 6. High-resolution frequency plotted against time for a violin executing vibrato. Symbols have the same meanings as in Fig. 5.

TABLE I. Error in quadratic fit calculation. The first column is the position of the true maximum of the function relative to zero. The second column is the position of the maximum predicted by the quadratic fit in Eq. (6), and the third column is the error in the quadratic fit calculation (difference in columns one and two).

$r$	$Q$ fit	Error
-0.500	-0.500	0.000
-0.400	-0.357	-0.043
-0.300	-0.247	-0.053
-0.200	-0.156	-0.044
-0.100	-0.076	-0.024
0.000	0.000	0.000
0.100	0.076	0.024
0.200	0.156	0.044
0.300	0.247	0.053
0.400	0.357	0.043
0.500	0.500	0.000

$$X[k] = \sum_{n=0}^{N-1} x[n] e^{-j2\pi kn/N},$$

where  $x[n] = e^{-j2\pi(k_0+r)n/N}$ . For the  $k_0^{\text{th}}$  bin we obtain

$$X[k_0] = e^{-j\pi r(N-1)/N} \frac{\sin(\pi r)}{\sin(\pi r/N)}.$$

For  $X[k_0+1]$ ,  $r \rightarrow r-1$  and for  $X[k_0-1]$ ,  $r \rightarrow r+1$  in the above expression.

We then use Eq. (2) to obtain the Hanning-windowed values for these Fourier coefficients,  $X^H[k_0]$ ,  $X^H[k_0+1]$  and  $X^H[k_0-1]$ . These three Fourier coefficients will be those having the maximum values and their amplitudes can be substituted in Eq. (5) to obtain the fractional value of  $k$  corresponding to the maximum of the parabola fitted through these three points.

$$\delta k = \frac{|X^H[k_0+1]| - |X^H[k_0-1]|}{2(|X^H[k_0]| - |X^H[k_0+1]| - |X^H[k_0-1]|)}. \quad (6)$$

Since the correct value is  $k_0+r$ , the error in the quadratic fit is then

$$r - \delta k.$$

We have carried out the calculation for values of  $r$  from  $-0.5$  to  $0.5$  and reported them in Table I along with the error in the value given by the quadratic fit which is the difference in the columns labeled  $r$  and  $Q$  fit. We also verified these values experimentally by generating a sinusoid with the appropriate  $r$ , carrying out a Hanning-windowed FFT analysis for 10 successive frames, and then determining the position of the maximum using the quadratic fit formula of Eq. (5). The results were identical to those given in column II of Table I with zero deviation among these results for different frames.

It should be noted that the error is independent of the bin number  $k_0$  so the fractional error which would be reported for an FFT would in fact be the error in the third column of Table I divided by  $k_0+r$ .

Our calculation based on phase differences from Eq. (4) was also applied to several of these frequencies. The

TABLE II. Comparison of average frequencies predicted by phase difference approximation (row two) and quadratic fit (row three) with their standard deviations from 10 measurements. Row one gives the exact frequencies in the test signal.

	Frequency	s.d.	Freq.	s.d.	Freq.	s.d.
True	133.506		267.012		400.518	
Phase approx.	133.505	0.654	267.009	1.277	400.514	1.036
Quad. fit	132.478	0.4155	265.138	0.771	398.214	0.151

deviation from the correct frequency was less than 0.01% with this method. We thus conclude that, for a signal consisting of a single component, the phase method is more accurate than the quadratic fit.

We then determined the effect of "spillover" from adjacent bins by generating a sound consisting of the sum of components in exact bin positions 3.1, 6.2, and 9.3. The results for 10 frames are found in Table II.

For this case the phase method again gives a more accurate value, but the standard deviation is greater. So the confidence in a single measurement would be lower for the phase method. It should be noted that the actual error is greater than the standard deviation for the quadratic fit.

## V. COMPARISON TO THE PHASE VOCODER

A comparison of this method with that of the phase vocoder is useful. It should be noted that there are two methods of conducting phase vocoder analyses. With the filterbank approach the sinusoidal analysis functions maintain a fixed phase with respect to the signal, and one measures deviations from center frequencies. On the other hand, the phase vocoder analysis is often carried out by taking FFT's, where the analysis functions do not maintain their initial phase with respect to the input signal, but rather restart at zero for each calculation. In this case the absolute phase is measured. To compensate, the phase change corresponding to the bin center frequency is subtracted from the measured phase change, or an equivalent method, such as circularly rotating samples in the analysis window, is applied. There are, nevertheless, errors in bins far removed from the bins in which components of the signal actually fall unless the hop size is 1. These errors increase as the hop size increases so there is a tradeoff between data proliferation and accuracy.

Our method is equivalent to a phase vocoder analysis using the FFT method with a hop size of 1 sample. The advantage is that we use the approximation of Eq. (3) and do not have to perform the second FFT. Thus we measure the absolute frequency for each bin, and get this information from a single FFT. With our method we obtain the exact frequency of the source for five or so bins on either side of the bin with center frequency closest to that of the

input sinusoidal component. Our method has clear advantages over the conventional phase vocoder and thus holds promise for musical synthesis as well as analysis.

## VI. CONCLUSION

Our method of tracking the fundamental frequency of musical passages in real time is extremely accurate and reports frequencies to the nearest quarter tone. Our high resolution frequency determination can be used as a back end for a fundamental frequency tracker where high precision is desired. Applications range from analysis of sounds with continuous frequency variation to determination of temperament for performance studies in cognitive psychology.

## ACKNOWLEDGMENTS

ICB is grateful to IRCAM for their hospitality during a Sabbatical leave when much of this work was carried out and to Wellesley College for its generous Sabbatical leave policy. She would like to thank Dan Ellis of the MIT Media Lab for invaluable and illuminating conversations. Finally she is grateful to Jim Beauchamp of the University of Illinois for many helpful e-mail discussions.

- Beauchamp, J. W. (1966). "Transient Analysis of Harmonic Musical Tones by Digital Computer," Audio Eng. Soc. Preprint No. 479.
- Beauchamp, J. W. (1969). "A Computer System for Time-Variant Harmonic Analysis and Synthesis of Musical Tones," *Music by Computers*, edited by von Foerster and Beauchamp (Wiley, New York), pp. 19-61.
- Brown, J. C. (1991). "Calculation of a constant  $Q$  spectral transform," *J. Acoust. Soc. Am.* **89**, 425-434.
- Brown, J. C. (1992). "Musical fundamental frequency tracking using a pattern recognition method," *J. Acoust. Soc. Am.* **92**, 1394-1402.
- Brown, J. C., and Puckette, M. S. (1992). "An efficient algorithm for the calculation of a constant  $Q$  transform," *J. Acoust. Soc. Am.* **92**, 2698-2701.
- Charpentier, F. J. (1986). "Pitch Detection Using the Short-Term Phase Spectrum," *Proceedings of the International Conference on Acoustics, Speech, and Signal Processing* (IEEE, New York), pp. 113-116.
- Dolson, M. (1986). "The Phase Vocoder: A Tutorial," *Comput. Music J.* **10**, 14-27.
- Flanagan, J. L., and Golden, R. M. (1966). "Phase Vocoder," *Bell Syst. Tech. J.* **45**, 1493-1509.
- Friedman, D. (1985). "Instantaneous-Frequency Distribution vs Time: An Interpretation of the Phase Structure of Speech," *Proceedings of the International Conference on Acoustics, Speech, and Signal Processing*, (IEEE, New York), pp. 1121-1124.
- Grey, J. M., and Moorer, J. A. (1977). "Perceptual evaluations of synthesized musical instrument tones," *J. Acoust. Soc. Am.* **62**, 454-462.
- Moorer, J. A. (1978). "The Use of the Phase Vocoder in Computer Music Applications," *J. Audio Eng. Soc.* **26**, 42-45.
- Oppenheim, A. V., and Luis, J. S. (1981). "The Importance of Phase in Signal," *Proc. IEEE* **69**, 529-541.
- Oppenheim, A. V., and Schaffer, R. W. (1975). *Digital Signal Processing* (Prentice-Hall, Englewood Cliffs, NJ).
- Smith, J. O., and Serra, X. (1987). "An Analysis/Synthesis Program for Non-Harmonic Sounds Based on a Sinusoidal Representation," *Proceedings of the 1987 International Computer Music Conference* (Int. Computer Music Assoc., San Francisco), pp. 290-297.